



# Dislocation mobility versus dislocation substructure controlled deformation of icosahedral Al–Pd–Mn single quasicrystals

U. Messerschmidt <sup>a,\*</sup>, B.V. Petukhov <sup>b</sup>, M. Bartsch <sup>a</sup>, Ch. Dietzsch <sup>a</sup>, B. Geyer <sup>a</sup>,  
D. Häussler <sup>a</sup>, L. Ledig <sup>a</sup>, M. Feuerbacher <sup>c</sup>, P. Schall <sup>c</sup>, K. Urban <sup>c</sup>

<sup>a</sup> Max Planck Institute of Microstructure Physics, Weinberg 2, Halle (Saale) D-06120, Germany

<sup>b</sup> Institute of Crystallography, Russian Academy of Sciences, Moscow 117333, Russia

<sup>c</sup> Institute of Solid State Research, Research Centre Jülich, Jülich D-52425, Germany

## Abstract

This paper compares new high-voltage electron micrographs of the dislocation structure of icosahedral Al–Pd–Mn specimens deformed at a high temperature ( $\cong 800^\circ\text{C}$ ) with those deformed at a low temperature ( $610^\circ\text{C}$ ). At all temperatures, the dislocations consist of almost straight segments on different planes. However, planar faults trailed by the dislocations have been observed at low temperatures only. The temperature dependence of the steady-state flow stress is modelled based on an evolution law of the dislocation density proposed before including recovery, and by considering the contribution of long-range dislocation interactions to the flow stress. Owing to the thermally activated recovery of the microstructure, the activation energy of deformation measured experimentally turns out to be higher than the energy of the dislocation mobility, explaining the unreasonably high experimental values. © 2001 Elsevier Science B.V. All rights reserved.

*Keywords:* Plastic deformation; Quasicrystals; Recovery; Transmission electron microscopy

## 1. Introduction

Since it became possible to grow large single quasicrystals of icosahedral Al–Pd–Mn, the intrinsic deformation behaviour of quasicrystals has been studied in some detail on this material (e.g. Ref. [1]). The first results on the temperature and strain-rate dependence of the flow stress have been interpreted in terms of the dislocation mobility [2]. A cluster friction model has been established [3] and formulated in a more quantitative way to explain the experimental values of the activation volume [4]. Recently, it was argued that the activation parameters at low temperatures can also be explained in terms of a Peierls model [5], which had been proposed before [6]. However, transient effects arising during changes of the deformation conditions as well as a strong decrease of the density of deformation-induced dislocations during annealing at the deformation temperature [7] showed that recovery processes during deformation cannot be neglected. It was concluded in Ref. [8] that the consider-

ation of recovery is necessary to explain the observed deformation curves [2,9] with a yield drop followed by a range of almost steady-state deformation. Only at low temperatures, where a steady state is not achieved, should deformation be controlled mainly by the dislocation mobility [10]. The brittle-to-ductile transition between both ranges occurs at about  $630^\circ\text{C}$  at a deformation rate of  $10^{-5} \text{ s}^{-1}$  [9]. The present paper presents new results on the dislocation microstructure of deformed Al–Pd–Mn single quasicrystals obtained in a high-voltage electron microscope (HVEM), which allows the imaging of the spatial arrangement of the dislocations. In addition, results of model calculations on the temperature and strain rate dependences of the steady-state flow stress are reported in which the effect of recovery on the athermal contribution to the flow stress is included.

## 2. Dislocation structure of deformed specimens

Icosahedral Al–Pd–Mn single quasicrystals have been deformed in compression in air at different temperatures and strain rates. To reduce the influence of recovery during cooling, specimens deformed at high

\* Corresponding author. Tel.: +49-345-5582927; fax: +49-345-5511223.

E-mail address: um@mpi-halle.de (U. Messerschmidt).

temperatures have been cooled under almost full load down to about 630°C, where recovery is very slow. Fig. 1 shows the typical dislocation structure at 610°C, i.e. in the low-temperature range, where plastic deformation is mainly achieved during stress relaxation tests. The dislocations are almost straight and arranged along crystallographic orientations on crystallographic planes. Very frequently, individual segments of the same dislocation belong to different planes. This is a prerequisite to dislocation multiplication as described before [5]. At low temperatures, slip is concentrated in rather narrow slip bands. Part of the dislocations trail planar faults marked by fringe contrast. Fig. 2 is a stereo pair of the structure after deformation at high temperatures. The main differences are that planar faults do not occur, that the dislocations are now distributed quite uniformly and that they form a spatial network with a link length of the order of 1  $\mu\text{m}$ .

### 3. Modelling of plastic deformation

In order to improve the understanding of the plastic deformation of Al–Pd–Mn quasicrystals, particularly

the observation of very high activation energies, the deformation is modelled based on equations similar to those discussed in Ref. [8]. These equations do not involve anything particular for quasicrystals but yield results that are consistent with the dislocation densities,  $\rho$ , measured in Ref. [7]. The plastic strain rate,  $\dot{\epsilon}_{\text{pl}}$ , is related to the dislocation velocity,  $v$ , by the Orowan relation

$$\dot{\epsilon}_{\text{pl}} = \rho b v \quad (1)$$

where  $b$  is the absolute value of the Burgers vector. The evolution of the dislocation density may be described by

$$d\rho/dt = w\tau^*\rho v - q\rho^2 \quad (2)$$

taking into account the dislocation multiplication with a rate constant,  $w$ , and annihilation with a rate constant,  $q$ . Eq. (2) equals equation 15 in Ref. [8], except that here, the total stress,  $\tau$ , is replaced by the effective stress,  $\tau^*$ , according to

$$\tau = \tau_i + \tau^* \quad (3)$$

where  $\tau_i$  is the long-range internal stress component. As the diffusion of atoms is involved in the process of recovery,  $q$  may depend strongly on the temperature with

$$q = q_0 \exp(-\Delta H_r/kT). \quad (4)$$



Fig. 1. Dislocation structure after deformation at 610°C. Strain rate  $10^{-6} \text{ s}^{-1}$ , plastic strain 0.6%, twofold compression axis, pseudo-twofold beam direction.

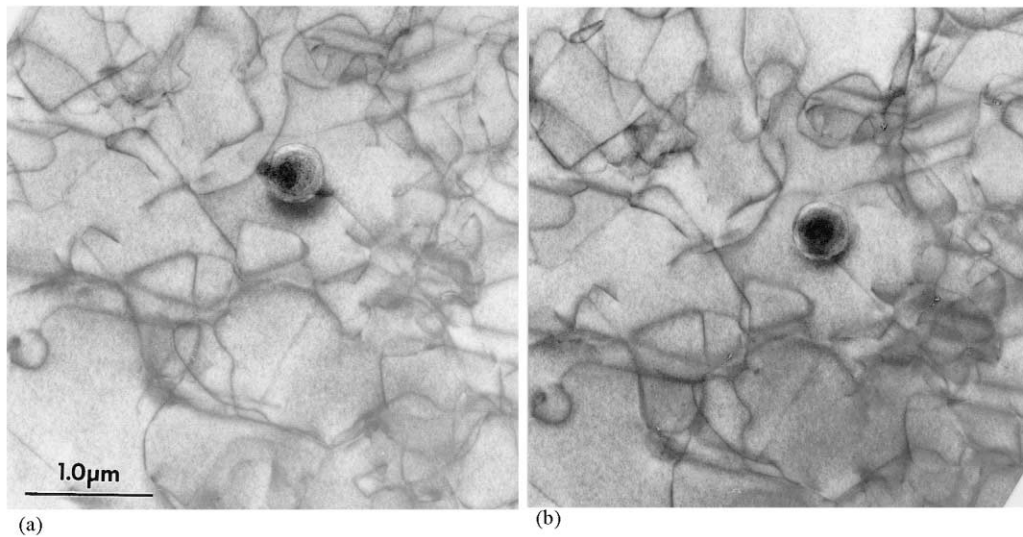


Fig. 2. Stereo pair of a dislocation network after deformation at 818, 797 and 777°C. Strain rate  $10^{-5} \text{ s}^{-1}$ , plastic strain 4.5%, fivefold compression axis, fivefold beam direction. A number of dislocations forming the network are extinguished.

Here,  $q_0$  is a preexponential factor,  $\Delta H_r$ , the activation enthalpy of recovery,  $k$ , the Boltzmann constant, and  $T$ , the absolute temperature. The relation between the plastic strain rate,  $\dot{\epsilon}_{pl}$ , of Eq. (1), and the total strain rate,  $\dot{\epsilon}$ , is described by the machine equation

$$(1/S)(d\tau/dt) = \dot{\epsilon} - \rho bv, \quad (5)$$

with  $S$  being the elastic modulus of the specimen and the grips. The dislocation velocity is represented by a power law instead of the Arrhenius law in Ref. [8]

$$v = v_0 \tau_m^* \exp(-\Delta G_m/kT), \quad (6)$$

where  $v_0$  is a preexponential factor,  $m$ , the so-called stress exponent, and  $\Delta G_m$ , the Gibbs free energy at zero stress of the processes controlling the dislocation mobility. The internal stress is described by a formula of Taylor hardening

$$\tau_i = \alpha \mu b \rho^{1/2}. \quad (7)$$

Here,  $\alpha$  is a numerical constant between about 0.2 and 1, and  $\mu$  is the shear modulus.

Schematically, the stress–strain behaviour during the deformation at a constant strain rate,  $\dot{\epsilon}$ , is as follows. At the beginning, when the initial dislocation density,  $\rho_0$ , is low, the stress increases almost linearly with time,  $\tau \cong S\dot{\epsilon}t$ , as shown by Eq. (5), and the internal stress,  $\tau_i$ , is small almost up to the yield point. After the upper yield stress, a steady state of the deformation develops with the flow stress,  $\tau_{ss}$ . The steady-state solution of Eqs. (2), (3), (5)–(7) is

$$\rho_{ss} = \rho_c / D^{m/(2m+1)} \quad (8)$$

and

$$\tau_{ss} = \tau_c (D^{1/(2m+1)} + a / D^{m/(4m+2)}). \quad (9)$$

Here,  $\rho_c = (\dot{\epsilon}/(v_0 \exp(-\Delta G_m/kT)))^{2/(m+2)} (w/S)^{m/(m+2)}$  and  $\tau_c = (S\dot{\epsilon}/(wv_0 \exp(-\Delta G_m/kT)))^{1/(m+2)}$  are scaling factors of the dislocation density and the stress, while  $D$  and  $a$  are dimensionless parameters characterizing the effects of recovery

$$D = (q/b)(w/\dot{\epsilon})^{(m-1)/(m+2)} S^{-(2m+1)/(m+2)} \times (v_0 \exp(-\Delta G_m/kT))^{-3/(m+2)} \quad (10)$$

and hardening

$$a = \alpha \mu (bw/S)^{1/2}. \quad (11)$$

In Fig. 3a, theoretical curves are plotted together with experimental values of the steady-state stress. The curves correspond to a data set with  $\alpha = 1$ ,  $m = 4$ ,  $\Delta G_m = 3 \text{ eV}$ , and  $\Delta H_r = 4 \text{ eV}$ . The remaining parameters ( $v_0$ ,  $q_0$ ) have been chosen as to make Eq. (8) consistent with the measured dislocation densities at the lower yield point [7]. Fig. 3b demonstrates that the ratio between the internal stress component,  $\tau_i$ , and the total flow stress is about 0.8 at low temperatures but falls below 0.5 at high temperatures.

#### 4. Discussion

In Section 2, it is pointed out that planar faults are created by moving dislocations only at low temperatures. Up to now, neither the nature of these faults nor their role in controlling the macroscopic flow stress has been elucidated. In particular, there is no experimental evidence that their production would cause a large friction stress, which prevents plastic deformation at low temperatures and is responsible for the transition between the deformation ranges at about 630°C. Obviously, continuous

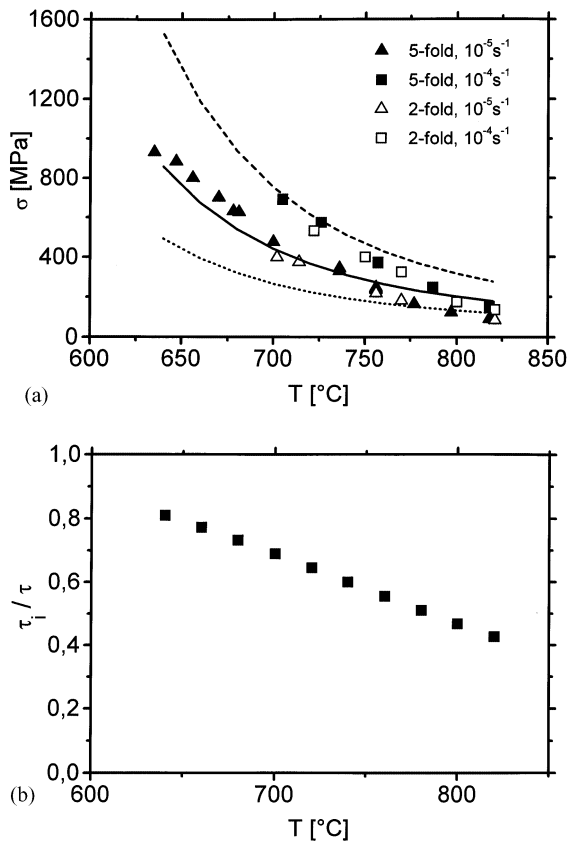


Fig. 3. Results of the modelling. (a) Temperature and strain-rate dependence of  $\tau_{ss}$  (lines) and experimental data from [9]. (b) Temperature dependence of  $\tau_i/\tau$  at  $\dot{\epsilon} = 10^{-5} \text{ s}^{-1}$ .

deformation with a yield drop and an almost steady-state range of deformation presupposes recovery of the dislocation structure. This means that the athermal stress component,  $\tau_i$ , cannot be neglected, as discussed already in Refs. [8,9]. The arrangement of the dislocations in a three-dimensional network shown in Fig. 2 fits the model of recovery-controlled deformation at high temperatures. However, the link length of  $1 \mu\text{m}$  is certainly too large to explain the whole  $\tau_i$  via a link length model.

The plastic deformation of quasicrystals has been modelled previously [11], using somewhat different equations. The present model does not consider any special feature typical of quasicrystals. Thus, it does not describe the softening observed at large strains. There is the general problem of how to interpret the high experimental activation energies,  $\Delta G_{\text{ex}}$ , at high temperatures. The experimental Gibbs free energy at non-zero stress is about 3.5 eV, and the work term amounts to about 0.4 eV (e.g. Refs. [2,8]). Thus,  $\Delta G_{\text{ex}} \cong 4 \text{ eV}$ . At low temperatures, where recovery can be neglected and the present model cannot be applied,  $\Delta G_{\text{ex}}$  is about 2.2 eV [8,10], which should be close to  $\Delta G_m$ . In the present model, the effective activation energy  $\Delta G_{\text{ex}}$  depends on the activation energy of the dislocation mobility  $\Delta G_m$  and of the recovery  $\Delta H_r$ . According to the dislocation density data

in Ref. [7],  $\Delta H_r$  is about 4 eV [7,8] although, as discussed in Ref. [8], this value is remarkably higher than the energy of self-diffusion. If the first term in Eq. (9), i.e.  $\tau^*$ , dominates the deformation, the effective activation energy is  $\Delta G_{\text{ex}} = 2\Delta G_m - \Delta H_r$ , which was concluded already in Ref. [8]. However, if the second term of Eq. (9), i.e.  $\tau_i$ , dominates, then  $\Delta G_{\text{ex}} = (\Delta G_m + m\Delta H_r)/(m + 1)$ . Thus, the present model can explain a transition of the experimental activation energy  $\Delta G_{\text{ex}}$  from a low value in the low-temperature range where recovery can be neglected to a higher value in the high-temperature range if recovery is taken into account, if  $\Delta H_r > \Delta G_m$ , and if  $\tau_i$  dominates the deformation. In the present case,  $\Delta G_{\text{ex}} \cong 3.4 \text{ eV}$ . The used set of parameters is consistent with the dislocation density data and with the experimental strain-rate sensitivity. It does not exactly describe the experimental temperature dependence of the flow stress. Its strong temperature dependence would be better described by higher activation energies  $\Delta G_m$  and  $\Delta H_r$ , which, however, are not in agreement with the other experimental data. Nevertheless, in spite of its shortcomings, the results of this very simple model are in fair agreement with all experimental data on the steady-state plastic deformation of Al–Pd–Mn quasicrystals, and it gives a clue as to how the high experimental activation energies can be interpreted. For an understanding of the transient effects, a more sophisticated model has to be developed.

## Acknowledgements

The authors thank the Deutsche Forschungsgemeinschaft for financial support.

## References

- [1] M. Wollgarten, M. Beyss, K. Urban, H. Liebertz, U. Köster, Phys. Rev. Lett. 71 (1993) 549.
- [2] M. Feuerbacher, B. Baufeld, R. Rosenfeld, M. Bartsch, G. Hanke, M. Beyss, M. Wollgarten, U. Messerschmidt, K. Urban, Phil. Mag. Lett. 71 (1995) 91.
- [3] M. Feuerbacher, C. Metzmaker, M. Wollgarten, K. Urban, B. Baufeld, M. Bartsch, U. Messerschmidt, Mater. Sci. Eng. A 233 (1997) 103.
- [4] U. Messerschmidt, M. Bartsch, M. Feuerbacher, B. Geyer, K. Urban, Phil. Mag. A 79 (1999) 2123.
- [5] U. Messerschmidt, D. Häussler, M. Bartsch, B. Geyer, M. Feuerbacher, K. Urban, Mater. Sci. Eng. A 294-296 (2000) 757.
- [6] S. Takeuchi, T. Hashimoto, Jpn. J. Appl. Phys. 22 (1993) 2063.
- [7] P. Schall, M. Feuerbacher, M. Bartsch, U. Messerschmidt, K. Urban, Phil. Mag. Lett. 79 (1999) 785.
- [8] U. Messerschmidt, M. Bartsch, B. Geyer, M. Feuerbacher, K. Urban, Phil. Mag. A 80 (2000) 1165.
- [9] B. Geyer, M. Bartsch, M. Feuerbacher, K. Urban, U. Messerschmidt, Phil. Mag. A 80 (2000) 1151.
- [10] U. Messerschmidt, B. Geyer, M. Bartsch, M. Feuerbacher, K. Urban, Mater. Res. Soc. Symp. Proc. 553 (1999) 319.
- [11] P. Guyot, G. Canova, in: S. Takeuchi, T. Fujiwara (Eds.), Quasicrystals, World Scientific, Singapore, 1998, p. 529.